Structural characterization of three-component Fibonacci Ta/Al multilayer films

R. W. Peng, A. Hu, S. S. Jiang, C. S. Zhang, and D. Feng
Laboratory of Solid State Microstructures, Nanjing University, Nanjing 210 008, People's Republic of China
(Received 31 January 1992; revised manuscript received 22 May 1992)

A new class of quasiperiodic superlattice structures called three-component Fibonacci structures has been studied both theoretically and experimentally. These structures with the characteristic irrational intervals A, B, and C can be produced by the substitution rule $A \rightarrow AC$, $C \rightarrow B$, and $B \rightarrow A$. The projection method is applied to deal with the pattern and index of their diffraction spectrum. The analytical results are compared with the experimental one from three-component Fibonacci Ta/Al superlattices. The experimental results are in good agreement with the numerical calculations using the model for compositionally modulated multilayers. Some possible applications of these structures are discussed.

I. INTRODUCTION

In recent years experimental and theoretical studies[1-7] on one-dimensional (1D) aperiodic systems have been made. The interest stems partly from the discovery of quasicrystals in 1984 by Schechtman *et al.*[1] Although quasicrystals are perfectly ordered, however, because there is no translational symmetry, they cannot be described in the usual terms of Bravais lattices and the Bloch theorem is inapplicable. On the other hand, the wave functions are not all exponentially localized as in the 1D disordered system. In some senses, quasicrystals can be regarded as an intermediate case between periodic and disordered solids. Due to the fact that 1D quasiperiodic structures are much simpler than three-dimensional (3D) quasicrystals, and that moreover the characteristic interval and growth sequence in 1D quasiperiodic structures can be intentionally chosen, studies on quasiperiodic superlattices are useful to gain information about the physical properties of quasicrystalline materials.

One of the well-known examples in 1D quasiperiodic sequences is the Fibonacci sequence. The Fibonacci sequence can be produced by repeated application of the substitution rule $A \rightarrow AB$ and $B \rightarrow A$. The ratio of the two commensurate intervals is equal to the golden mean $\tau=(\sqrt{5}+1)/2$. In 1985, Merlin *et al.*[4] reported a realization of Fibonacci GaAs-AlAs superlattices. Since then, many experiments on aperiodic superlattices have been made. To our knowledge, most of these experiments[5-7] were based on Fibonacci superlattices and only a few experiments have been performed on non-Fibonacci structures. For example, Thue-Morse superlattices were investigated by Raman scattering[8] and by high-resolution x-ray diffraction.[9] Thue-Morse sequences can be generated by dual automation and the substitution rule $A \rightarrow AB$ and $B \rightarrow BA$. Their behavior is intermediate between quasiperiodicity and randomness. The other example is the investigation on quasiperiodic superlattices reported by Birch *et al.*[10] Their inflation rule is $A \rightarrow A^m B$ and $B \rightarrow A$ (where m is an integer). Generally speaking, all these 1D aperiodic structures consist only of two building blocks, A and B, with different generation sequences. Actually, according to the procedure of superlattices, both the number of building blocks and the growth sequence can chosen intentionally, which gives rise to the construction of new structures of superlattices.

In this paper, the diffraction properties of a new class of 1D quasiperiodic structures called three-component Fibonacci structures (3CFS's) are investigated both theoretically and experimentally. The 3CFS's can be generated by the inflation rule $A \rightarrow AC$, $C \rightarrow B$, and $B \rightarrow A$, where A, B, and C are three building blocks. The ratios between the intervals d_B, d_A and between the intervals d_C, d_A are special irrational ξ and η, which satisfy the equations $\eta^3+\eta-1=0$ and $\xi=\eta^2$. In Sec. II, the projection method is applied to deal with the diffraction pattern. The diffraction vector is given by $q=2\pi D^{-1}(n_1+n_2\xi+n_3\eta)$, where D is an average superlattice wavelength and n_i $(i=1,2,3)$ are integers. In Sec. III, the fabrication and structural characterization of three-component Fibonacci (3CF) Ta/Al multilayers are reported. The numerical calculations are carried out using the model for the compositionally modulated multilayers. Finally, some possible applications are discussed.

II. THEORETICAL MODELS

The procedure to generate what we called three-component Fibonacci structures involves two steps: first, we define a basis which includes three distinct building blocks A, B, and C. Then, we order these building blocks in a three-component Fibonacci sequence, i.e., the substitution rule is described by $A \rightarrow AC$, $C \rightarrow B$, and $B \rightarrow A$. Obviously, this rule can be expressed by a 3×3 matrix M, that is,

$$\begin{bmatrix} A \\ B \\ C \end{bmatrix} \rightarrow M \begin{bmatrix} A \\ B \\ C \end{bmatrix}, \tag{1}$$

where

$$M=\begin{bmatrix} 1 & 0 & 1 \\ 1 & 0 & 0 \\ 0 & 1 & 0 \end{bmatrix}.$$

On the other hand, 3CFS can be described as the limit of generations S_r which obeys the rule $S_r=S_{r-1}+S_{r-3}$ with $S_1=\{A\}$, $S_2=\{AC\}$, and $S_3=\{ACB\}$. If $N_r(A)$, $N_r(B)$, and $N_r(C)$ represent the numbers of A, B, and C in S_r, respectively, and if two ratios of these numbers are denoted by $\eta=\lim_{r\to\infty}[N_r(C)/N_r(A)]$ and $\xi=\lim_{r\to\infty}[N_r(B)/N_r(A)]$, the ratios satisfy the following equations:

$$\eta^3+\eta=1 ,$$
$$1:\eta=\eta:\xi . \tag{2}$$

Then we obtain the values of η and ξ:

$$\eta=[1/2+1/2(31/27)^{1/2}]^{1/3}+[1/2-1/2(31/27)^{1/2}]^{1/3} ,$$
$$\xi=-2/3+[29/54+1/2(31/27)^{1/2}]^{1/3}+[29/54-1/2(31/27)^{1/2}]^{1/3} .$$

It is obvious that η and ξ are irrational numbers between 0 and 1. One should note, η is just the reciprocal of the characteristic root λ ($\lambda>1$) of the characteristic equation $x^3-x^2-1=0$ of matrix M.

A low-dimensional quasiperiodic structure may be regarded as the projection of a high-dimensional periodic structure.[11,12] In our case, since the characteristic polynomial of the substitution rule has only one root λ of absolute value greater than 1, according to the Bombieri-Taylor theorem,[13] the 3CFS's are available by the projection method, i.e., by projecting a three-dimensional periodic structure along a line. Consider a cubic lattice with unit spacing in three-dimensional space. Set up an orthogonal coordinate system, where the point O is the origin and $\mathbf{x}_i$ ($i=1,2,3$) are axes. Let the axis $\mathbf{x}_3'$ be a projecting line, and the three axes $\mathbf{x}_1'$, $\mathbf{x}_2'$, $\mathbf{x}_3'$ with the same origin O constitute another orthogonal coordinate system. Let the angle between $\mathbf{x}_j'$ and $\mathbf{x}_i$ ($i,j=1,2,3$) be α_{ji}. If the projection axis $\mathbf{x}_3'$ satisfies

$$\cos\alpha_{31}:\cos\alpha_{32}:\cos\alpha_{33}=1:\xi:\eta , \tag{3}$$

where ξ and η are irrational numbers as mentioned above, then the set of projected points on the axis $\mathbf{x}_3'$ can construct an aperiodic 3CFS. The three intervals d_A, d_B, and d_C of 3CFS satisfy

$$d_A:d_B:d_C=\cos\alpha_{31}:\cos\alpha_{32}:\cos\alpha_{33}=1:\xi:\eta . \tag{4}$$

Additionally, the cubic lattice may be represented by the function

$$U_0(x_1,x_2,x_3)=1/(8\pi^3)\sum\delta(x_1-i)\delta(x_2-j)\delta(x_3-k) , \tag{5}$$

where the sum is all the integers (i,j,k), and the projection function is

$$R(x_1',x_2')=\begin{cases}1 & (\text{if } |x_1'|\le\omega_0,\ |x_2'|\le v_0)\\ 0 & (\text{otherwise}) .\end{cases} \tag{6}$$

Thus, the sum of points of 3CFS can be represented by

$$Q(x_3')=\int_{-\infty}^{+\infty}\int R(x_1',x_2')U_0(x_1',x_2',x_3')dx_1'dx_2' , \tag{7}$$

$$U_0(x_1',x_2',x_3')=U_0\left[\sum_{i=1}^{3}x_i'\cos\alpha_{i1},\ \sum_{i=1}^{3}x_i'\cos\alpha_{i2},\ \sum_{i=1}^{3}x_i'\cos\alpha_{i3}\right] . \tag{8}$$

It is well known that the diffraction pattern of a lattice is simply related to the Fourier transformation of a lattice. Using $S(p,k)$ and $M(x_3',p,k)$ as the transformation of R and U, respectively, and according to the convolution law, we have

$$Q(x_3')=\int\int dp\,dk\,S(-p,-k)M(x_3',p,k) . \tag{9}$$

Here, we are interested in the Fourier transformation $F(q)$ of $Q(x_3')$, thus the following relation holds:

$$F(q)=\int\int dp\,dk\,S(-p,-k)V(q,p,k) , \tag{10}$$

$$V(q,p,k)=\sum\delta(k-2\pi k(n_1,n_2,n_3))\times\delta(p-2\pi p(n_1,n_2,n_3))\times\delta(q-2\pi q(n_1,n_2,n_3)) , \tag{11}$$

$$S(p,k)=4\sin(p\omega_0)\sin(kv_0)/(pk) . \tag{12}$$

Therefore, Eq. (10) can be rewritten as

$$F(q)=\sum S(p(n_1,n_2,n_3),k(n_1,n_2,n_3))\times\delta(q-q(n_1,n_2,n_3)) , \tag{13}$$

$$k(n_1,n_2,n_3)=\begin{vmatrix} n_1 & \cos\alpha_{21} & \cos\alpha_{31}\\ n_2 & \cos\alpha_{22} & \cos\alpha_{32}\\ n_3 & \cos\alpha_{23} & \cos\alpha_{33}\end{vmatrix} , \tag{14}$$

$$p(n_1,n_2,n_3)=\begin{vmatrix} \cos\alpha_{11} & n_1 & \cos\alpha_{31}\\ \cos\alpha_{12} & n_2 & \cos\alpha_{32}\\ \cos\alpha_{13} & n_3 & \cos\alpha_{33}\end{vmatrix} , \tag{15}$$

$$q(n_1,n_2,n_3)=\begin{vmatrix}\cos\alpha_{11} & \cos\alpha_{21} & n_1\\ \cos\alpha_{12} & \cos\alpha_{22} & n_2\\ \cos\alpha_{13} & \cos\alpha_{23} & n_3\end{vmatrix} . \quad (16)$$

The corresponding equation for the orthonormal condition is

$$\begin{vmatrix}\cos\alpha_{11} & \cos\alpha_{21} & \cos\alpha_{31}\\ \cos\alpha_{12} & \cos\alpha_{22} & \cos\alpha_{32}\\ \cos\alpha_{13} & \cos\alpha_{23} & \cos\alpha_{33}\end{vmatrix}=1 . \quad (17)$$

Considering Eqs. (4) and (17), it is possible to rewrite Eq. (16) as

$$q(n_1,n_2,n_3)=2\pi D^{-1}(n_1+n_2\xi+n_3\eta) , \quad (18)$$

$$D=1/\cos\alpha_{31}=d_1+d_2\xi+d_3\eta , \quad (19)$$

where n_1,n_2,n_3 are integers and D is the average lattice wavelength.

Equation (13) displays clearly the diffraction spectrum of 3CFS. First, the location of diffraction peaks are shown and $q(n_1,n_2,n_3)$ is the diffraction vector. According to Eq. (18), each peak can be labeled by three indices

$$\begin{bmatrix}n_1\\ n_2\\ n_3\end{bmatrix} .$$

Secondly, $S(p,k)$ is related to the intensity of the diffraction. The intensities are proportional to the square of the absolute value of $S(p,k)$. It is easy to prove that the strongest peaks will satisfy

$$n_1:n_2:n_3\cong 1:\xi:\eta . \quad (20)$$

The indices of the strongest peaks correspond to a group of generalized Fibonacci numbers (a_n,a_{n-2},a_{n-1}). The numbers $\{a_n\}$ can be defined by

$$a_n=a_{n-1}+a_{n-3} ,$$
$$a_1=a_2=0, \quad a_3=1 . \quad (21)$$

Therefore, the strongest peaks reflect the self-similarity of reciprocal lattices as follows:

$$q(a_{n+3},a_{n+1},a_{n+2}) =q(a_{n+2},a_n,a_{n+1})+q(a_n,a_{n-2},a_{n-1}) . \quad (22)$$

To summarize this section, we conclude that 3CFS can be obtained by ordering three building blocks A,B,C in special sequences, and the peak positions of the lattice can be labeled by three integers

$$\begin{bmatrix}n_1\\ n_2\\ n_3\end{bmatrix} ,$$

which are given by Eq. (18). The strongest peaks display the self-similar hierarchy shown by Eq. (22).

In our treatment of 3CFS, specific irrational values of ξ and η are assumed, just like the case of the standard Fibonacci sequence in which τ is assumed to be the golden mean. Generalization of 3CFS to the case with arbitrary d_A, d_B, and d_C can be envisaged. Since a cube and a cuboid are topologically equivalent, a nonstandard 3CF lattice, where $d_A:d_B:d_C\neq 1:\xi:\eta$, can be obtained by projecting from an orthogonal lattice instead of a cubic lattice, and Eqs. (18), (19), and (22) still hold. Thus the nonstandard 3CF lattice is still quasiperiodic.

III. SAMPLE PREPARATION AND CHARACTERIZATION

The three-component Fibonacci Ta/Al multilayer films were fabricated on a glass substrate by dual-target magnetron sputtering. The vacuum system was initially pumped down to 5×10^{-6} Torr. During sputtering, the argon gas pressure was kept constant at 7.0 mTorr. Pure Ta and Al targets (with diameters of 2.36 in.) were used. During the process, the substrates can be alternately rotated at three speeds to be exposed to individual magnetron sources comprised of Ta and Al targets. The parameters of the structure were chosen so that Ta slabs of the same thickness were separated by three different slabs of Al. In a typical sample, the building blocks A, B, and C consisted of (12.7 Å Ta)-(36.44 Å Al), (12.7 Å Ta)-(9.89 Å Al), and (12.7 Å Ta)-(21.11 Å Al), respectively. The ratios d_B/d_A and d_C/d_A were approximately ξ and η, respectively. The average lattice parameter was $D=d_A+\xi d_B+\eta d_C=82.72$ Å. The sample we studied consisted of 16 generations of 3CFS. The total sample thickness was about 1.56 μm.

The multilayer films were characterized by x-ray diffractometry. A 12-kW Rigaku rotating anode x-ray source [a Cu anode in the high brilliance 0.2×2 mm^2 spot mode and a symmetric graphite (002) monochromator] was used. The measurements were made both near the Bragg peaks of Ta and Al at $2\theta=38.5°$ and at the grazing angles of incidence ($0.5°\leq 2\theta\leq 10.5°$). Both types of measurements are significant for the characterization of these samples. The scattering vector was kept normal to the surface for this diffraction pattern. In the high-angle region, the main diffraction peak was found [shown in Fig. 1(a)] representing the reflections from the bcc Ta(110) and fcc Al(111) planes which have an equal interlayer spacing of $a=0.2338$ nm. No other main peaks were found. This means that the sample is dominated by crystalline Ta and Al with a texture of Ta(110) and Al(111).[16] On both sides of the main Bragg reflection, 3CF satellite peaks were found. Considering the wave vector

$$q=4\pi/\lambda|\sin\theta_i-\sin\theta_0| \quad (23)$$

in the high-angle region (here, $2\theta_0=38.5°$), the locations of the satellite peaks are consistent with the result expressed by Eq. (18) in Sec. II. Thus the pattern from the 3CF samples takes three integers

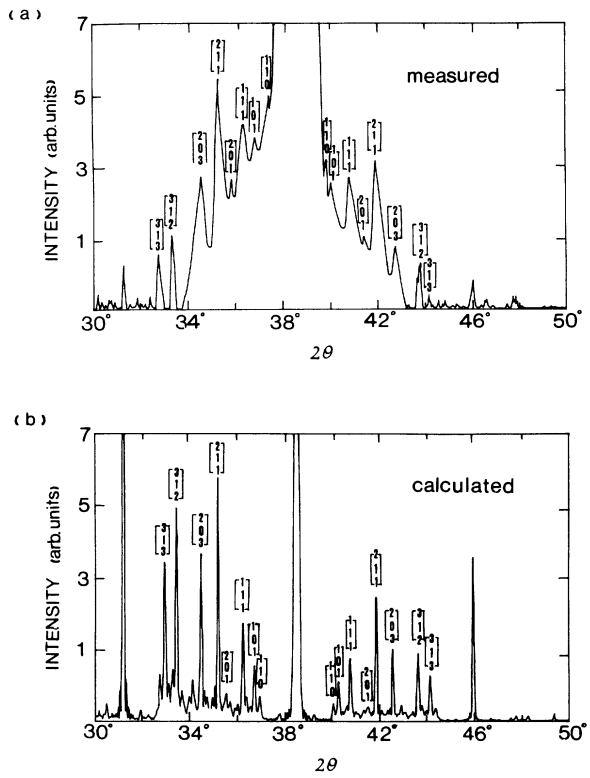

FIG. 1. The θ-2θ scan of x-ray diffraction in the high-angle region for 3CF Ta/Al multilayer with $D=82.72$ Å. Cu $K\alpha$ radiation. (a) Measured. (b) Calculated.

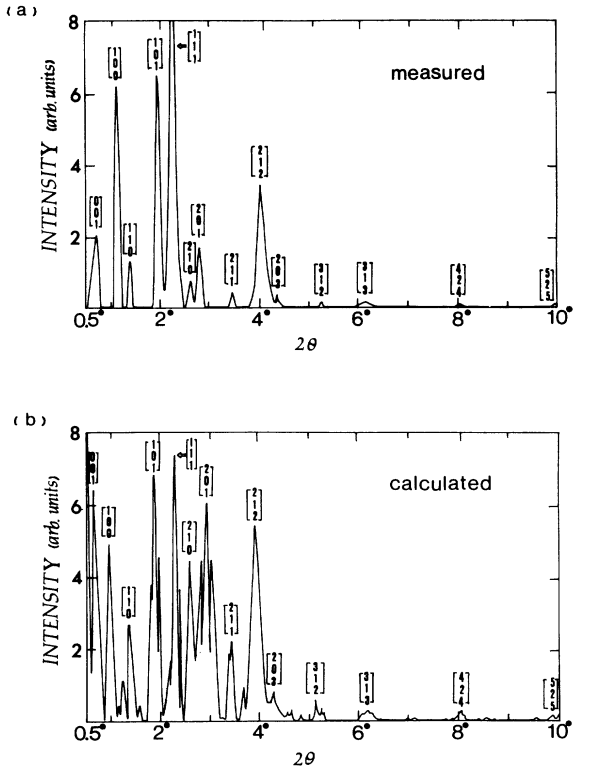

FIG. 2. The θ-2θ scan of x-ray diffraction in the low-angle region for 3CF Ta/Al multilayer with $D=82.72$ Å. Cu $K\alpha$ radiation. (a) Measured. (b) Calculated.

$$\begin{bmatrix} n_1 \\ n_2 \\ n_3 \end{bmatrix}$$

to label their positions [shown in Fig. 1(a)].

In the low-angle region, at least 14 harmonics have been observed [shown in Fig. 2(a)]. These 3CF peaks can also be indexed and labeled by

$$\begin{bmatrix} n_1 \\ n_2 \\ n_3 \end{bmatrix} .$$

Their relative intensities, peak positions, indices, and scattering vectors are listed in Table I. In Table I there are a few peaks with high relative intensities. The experimental values of the scattering vector agree remarkably well with the theoretical results based on Eq. (18). And the experimentally determined $q(n_1,n_2,n_3)$ satisfies the Eq. (22). It reflects the self-similarity of the reciprocal lattice. The diffraction peaks form a dense set. As compared with the results of the periodic Ta/Al structure,[14] five peaks have high relative intensities and the strongest peak of the 3CFS is not the nearest peak from $\theta=0$. It is the quasiperiodic order that gives rise to all these phenomena, which may be usable for special cases in soft x-ray and uv optics. On the other hand, compared with the results of the Fibonacci Ta/Al structure,[15] the locations of strong peaks in the diffraction pattern of 3CFS are more complex than those of the Fibonacci Ta/Al structure. The peaks of 3CFS must be indexed by three integers while the peaks of Fibonacci structure can be labeled only by two integers.

In order to obtain more information, the x-ray-diffraction patterns of 3CFS were numerically simulated. The model for the compositionally modulated multilayer was used. The calculation method was the same we used for the periodic Ta/Al (Ref. 14) and Fibonacci Ta/Al (Ref. 15) multilayer, except that the building blocks and the sequence were different. The results of the fitting calculation are shown in Figs. 1(b) and 2(b) where the degree of fluctuation in this sample is less than 9% and the coherence length perpendicular to the film is about 100 nm. The numerically calculated profiles are consistent with the experimental data for both relative scattering intensities and peak positions.

To conclude, two-target magnetron sputtering can be used to prepare 3CF Ta/Al superlattices. 3CFS can be obtained by the concurrent rule $A\rightarrow AC$, $C\rightarrow B$, and $B\rightarrow A$. The satellite peaks in the high-angle region and the strong peaks in the low-angle region in x-ray diffraction are analytically shown to occur for scattering vectors $q(n_1,n_2,n_3)=2\pi D^{-1}(n_1+\xi n_2+\eta n_3)$. A 1D quasiperiodic structure including three building blocks

TABLE I. Diffraction and calculation data in the low-angle region for a Ta/Al multilayer with $D=82.72$ Å. Cu $K\alpha$ radiation.

Index (n_1,n_2,n_3)	Peak position 2θ (deg)	Observed intensity (arb. units)	$q=4\pi\lambda_x^{-1}\sin\theta$ (Å^{-1})	$q=2\pi D^{-1}(n_1+n_2\xi+n_3\eta)$ (Å^{-1})
001	0.74	44 073	5.263×10^{-2}	5.182×10^{-2}
100	1.14	137 362	8.108×10^{-2}	7.595×10^{-2}
110	1.40	29 648	9.957×10^{-2}	0.1113
101	1.96	142 364	0.1394	0.1278
111	2.26	221 252	0.1607	0.1631
210	2.62	16 818	0.1863	0.1873
201	2.80	36 361	0.1991	0.2037
211	3.46	8 202	0.2461	0.2391
212	4.02	76 107	0.2859	0.2909
203	4.36	6 450	0.3100	0.3074
312	5.24	397	0.3726	0.3669
313	6.14	3 906	0.4365	0.4187
424	8.04	164	0.5714	0.5818
525	9.98	114	0.7089	0.7096

has been investigated in detail. We have performed a structural investigation of 3CFS's which is a 1D quasiperiodic structure with more than two incommensurate intervals both theoretically as well as experimentally. Similar to what was found for Fibonacci Ta/Al multilayers,[15] the 3CF Ta/Al multilayer belongs to the quasiperiodic high-Z and low-Z multilayers. From the diffraction pattern of 3CF Ta/Al multilayers, there is more than one strong peak in the low-angle region at a wavelength $\lambda_x=1.54$ Å. The structure may be used as a mirror with high normal-incidence reflectivity for soft x rays in synchrotron-radiation sources.

ACKNOWLEDGMENTS

We wish to thank G. Feng for his assistance with the experiments. This work was supported by the National Science Foundation of China.

[1]D. Schechtman, I. Blech, D. Gratias, and J. W. Cahn, Phys. Rev. Lett. **53**, 1951 (1984).
[2]S. Ostlund and R. Pandit, Phys. Rev. B **29**, 1394 (1984).
[3]D. Levine and P. J. Steinhardt, Phys. Rev. Lett. **53**, 2477 (1984).
[4]R. Merlin, K. Bajema, R. Clarks, F. Y. Juang, and P. K. Bhattacharga, Phys. Rev. Lett. **55**, 1768 (1985).
[5]J. Todd, R. Merlin, and Roy Clarke, Phys. Rev. Lett. **57**, 1157 (1986).
[6]A. Hu, C. Tien, X. Li, Y. Wang, and D. Feng, Phys. Lett. **A119**, 313 (1986).
[7]N. M. C. Dharma-wardana, A. H. MacDonald, D. J. Lockwood, J. M. Baribeau, and D. C. Houghton, Phys. Rev. Lett. **58**, 1761 (1987).
[8]R. Merlin, K. Bajema, J. Nagle, and K. Ploog, J. Phys. (Paris) Colloq. **48**, C5-503 (1987).
[9]Francoise Axel and Hikaru Terauchi, Phys. Rev. Lett. **66**, 2223 (1991).
[10]J. Birch, M. Severin, U. Wahlström, Y. Yamamoto, G. Radnoczi, R. Riklund, and J.-E. Sundgren, Phys. Rev. B **41**, 10 398 (1990).
[11]Veit Elser, Phys. Rev. B **32**, 4892 (1985).
[12]R. K. P. Zia and W. J. Dallas, J. Phys. A **18**, L341 (1985).
[13]E. Bombieri and J. E. Taylor, Contemp. Math. **64**, 241 (1987).
[14]S. S. Jiang, A. Hu, H. Chen, W. Liu, Y. X. Zhang, Y. Qiu, and D. Feng, J. Appl. Phys. **66**, 5258 (1989).
[15]R. W. Peng, A. Hu, and S. S. Jiang, Appl. Phys. Lett. **59**, 2512 (1991).
[16]S. S. Jiang, J. Zhou, D. J. H. Cockayne, A. Sikorski, A. Hu, and R. W. Peng, Philos. Mag. B (to be published).